

A Study on Multiple Steady States and Their Relation to Global Structure in Time Delayed Feedback Controlled Duffing System

Kohei YAMASUE[†] and Takashi HIKIHARA[†]

[†]Department of Electrical Engineering, Kyoto University
Katsura, Nishikyo, Kyoto 615-8510, Japan

Email: yamasue@dove.kuee.kyoto-u.ac.jp, hikihara@kuee.kyoto-u.ac.jp

Abstract—This paper concerns the bifurcation and origin of nontarget periodic orbits, which are unexpectedly stabilized under the time delayed feedback control of a two-well Duffing system. We reveal that the annihilation of the nontarget orbits by saddle-node bifurcation gives a criterion for the disappearance of the global structure governed by original chaos under the control.

1. Introduction

For more than a decade, controlling chaos has been an active research field in nonlinear science [1]. With taking a cue from the key concept proposed by Ott *et al.* [2], several advanced methods have been designed to stabilize unstable periodic orbits embedded in chaotic attractors. One of the strategies, called *time delayed feedback control*, is well-known as a practical method for controlling chaos [3]. This control method is easily applied to experimental systems, using only the difference signal between the present output signals and the past ones. The implementation does not need the exact model of the controlled object nor complicated computer processing for reconstruction of underlying dynamics. With these practical advantages, the control method has applications in various research fields; electronic circuits [4], laser systems [5], gas charge systems [6], mechanical oscillators [7], chemical systems [8] and so on. In addition, theoretical analysis has been developed on the basis of the stability analysis of the target unstable periodic orbits (see Ref. [9] and the references therein). One of the important results is the derivation of the odd number condition, which gives a class of unstable periodic orbits that cannot be stabilized by the control method and its extension [10, 11]. The odd number condition was first derived for discrete systems [12] and subsequently extended to continuous systems [13, 14]. Against this negative result, Pyragas improved the control method to circumvent the odd number condition [15].

On the other hand, the control method still has fundamental problems on the control performance related to the global dynamics of the controlled system [16]. We here note that the global dynamics of the controlled system is described by the structure of the phase space in function space, which has infinite dimension, since the controlled system is modeled by differential difference equations. With relevance to the global dynamics in function space, the authors have recently shown the domain of attraction

for stabilized orbits possibly has a self-similar structure in their boundaries [17]. They have also clarified the inheritance of the global chaotic dynamics from the original chaotic system has destructive influences on control performances, such as complicated domain of attraction and long chaotic transient behavior in the controlled systems [18]. These results clearly show that the global structure of the phase space should be considered for advanced use of the control method.

In this paper, we numerically discuss the multiple steady states in the time delayed feedback controlled two-well Duffing system. The two-well Duffing system is here considered as a model of the magnetoelastic system [19]. The controlling chaos of the two-well Duffing system is an important subject of research in engineering field, related to the elimination of the chaotic vibration in the mechanical systems. As the preceding results, the stabilization of the chaos in the magnetoelastic beam system was experimentally achieved [7]. The feature of the phase propagation of the control signal was discussed in Ref. [16]. Here we clarify the bifurcation and origin of the nontarget orbits obtained as steady states in the controlled system. We discuss the remain of the global chaotic dynamics based on the presence of nontarget orbits.

2. Two-well Duffing System under Time Delayed Feedback Control

The two-well Duffing system is a mathematical model describing the first-mode vibration in the magnetoelastic beam system under sinusoidal forcing [19]. The two-well Duffing system is here controlled by the signal $u(t)$:

$$\begin{cases} \dot{x}(t) = y(t) \\ \dot{y}(t) = -\delta y(t) + x(t) - x(t)^3 + A \cos \omega t + u(t), \end{cases} \quad (1)$$

where $x(t)$ and $y(t)$ denote the displacement and velocity of the two-well Duffing system, respectively. The control signal $u(t)$ is generated from the difference signal between the current output signal and past one. With measuring the velocity $y(t)$ as a output signal, the $u(t)$ is here obtained as follows:

$$u(t) = K[y(t - \tau) - y(t)], \quad (2)$$

where K implies the feedback gain. The τ denotes the time delay, which is adjusted to the period of the target unstable periodic orbits embedded in the chaotic attractor. Once

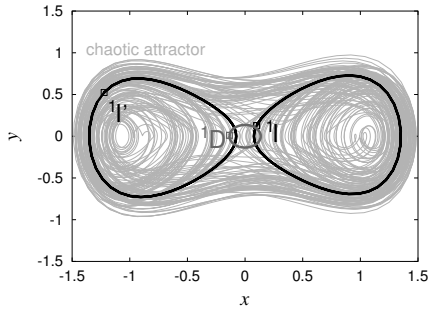


Figure 1: Unstable period- 2π orbits embedded in chaotic attractor. $1S'$ and $1S$ are target orbits. $1D$ cannot be stabilized due to odd number condition.

control turns on, the control signal converges to null, as the system is stabilized to one of the target orbits. As a result of the convergence, the controlled system degenerates from an infinite dimensional system with time delay to the original two dimensional system.

The parameter of the original system is here fixed at $(\delta, A, \omega) = (0.3, 0.34, 1.0)$, where the system generates the chaotic attractor [20]. δ denotes the damping coefficient. A represents the forcing amplitude and ω the frequency. The dynamics under $\omega = 1.0$ was summarized in [20]. τ is adjusted to 2π for stabilizing two symmetric inversely unstable periodic orbits with period- 2π , which are shown by $1S$ and $1S'$ in Fig. 1. One can easily confirm that the control signal stabilizes these orbits under certain amplitude of the feedback gain. The target orbits are here denoted by $1S$ and $1S'$, if they gain the stability under the control input. We note that the chaotic attractor has the other period- 2π orbit, which is a directly unstable periodic orbit denoted by $1D$ in Fig. 1. However, the orbit cannot be stabilized by the control method due to the odd number condition.

3. Coexisting Orbits

3.1. Convergence to Coexisting Orbits

Against the purpose of controlling chaos, the convergence to nontarget orbits unexpectedly occurs in the controlled Duffing systems [17]. We here introduce the convergence characteristics shown in Fig. 2. The convergence characteristics in Fig. 2(a) was numerically determined with the feedback gain shown by vertical axis and the onset time of control by horizontal axis. The shift of the onset time of control varies the initial condition of the controlled system because of the chaotic behavior before control turns on. The classification of tones is shown in Fig. 2(b). The classification does not distinguish the states with the same period for simplicity.

In Fig. 2, there is a dominant region where the state converges to the target period- τ orbits. However, nontarget orbits are also obtained as steady states, depending on the initial condition in function space. For example, one clearly observes the convergence to the coexisting period- 3τ orbits at $K \approx 0.935$ or the period- 6τ orbits within $0.9 \lesssim K \lesssim 0.93$. These nontarget orbits coexist with the

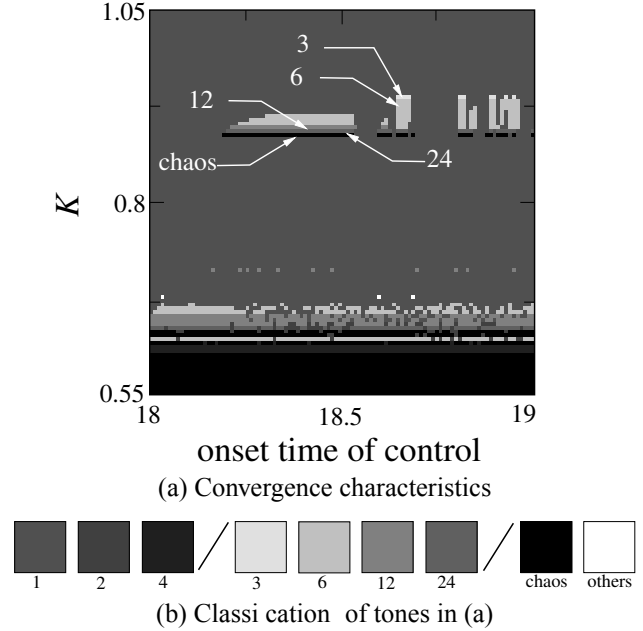


Figure 2: Convergence characteristics [17]

target orbits under the control input. The convergence to the coexisting orbits implies the failure of the control from the goal of controlling chaos.

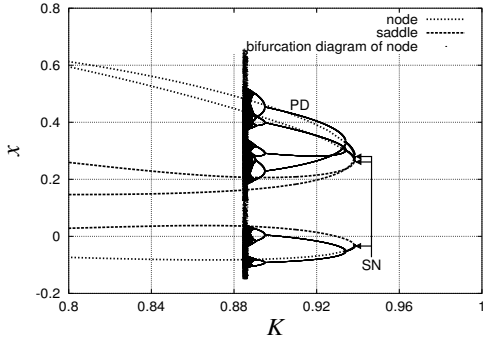
3.2. Bifurcation of Coexisting Orbits

This section gives an overview for the changes of the dynamical properties of the coexisting orbits. The bifurcation of the coexisting orbits is illustrated using one parameter bifurcation diagram provided by the successive change of the feedback gain.

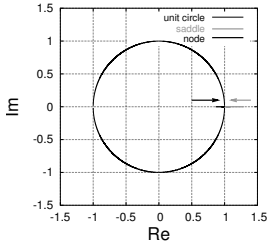
Figure 3(a) shows a bifurcation diagram for a coexisting period- 3τ orbit. The bifurcation diagram is shown by black points, which indicate stroboscopic observation of displacement x with period- τ . The diagram is obtained by monotonous increase and decrease of the feedback gain with sweeping from $K = 0.935$, at which the coexisting orbit is obtained as a steady state. The stability of the coexisting orbits is governed by the moduli of its characteristic multipliers.

3.2.1. Annihilation by Saddle-Node Bifurcation

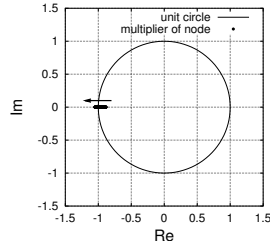
The coexisting orbit disappears at the upper limit of the stability range. This disappearance is governed by the saddle-node bifurcation with another unstable periodic orbit which makes a pair to the stable coexisting orbit. It is confirmed that a pair of characteristic multipliers reaches unity at the bifurcation point, shown in Fig.3(b). The pair of the multipliers annihilates on the unit circle after each multiplier reaches at unity from inside and outside of the unit circle, respectively. Though the orbits have an infinite number of multipliers because of the extension from two dimension to infinite dimension, we here call the stable orbit *node* and corresponding unstable one *saddle*. After the node and saddle coalesce and annihilate, both orbits no longer exist under the control input.



(a) Bifurcation diagram



(b) Annihilation of a pair of characteristic multipliers at saddle-node bifurcation point



(c) Characteristic multiplier outgoing through -1 at period-doubling bifurcation point

Figure 3: Bifurcation of coexisting period- 3τ orbit

3.2.2. Loss of Stability by Period-Doubling Bifurcation

At the lower limit of the stability range, the node loses the stability and then bifurcates to a period- 6τ orbit under the period-doubling bifurcation. In Fig. 3(a), we can see that each of three branches originating from the saddle-node bifurcation point generates a pair of branches for the decrease of the feedback gain. One of the characteristic multipliers leaves unit circle across -1 , as shown in Fig. 3(c). The continuous decrease of the feedback gain make period-doubling bifurcation successively occur, as shown in Fig. 3(a). It yields period- 12τ , period- 24τ coexisting orbits. After the accumulation of the period-doubling, finally a coexisting chaotic attractor generated.

The generated chaotic attractor persists and coexists with the stable target orbits if the feedback gain slightly decreases. However, this chaotic attractor is suddenly destroyed as the feedback gain continues to decrease. Then multiple steady states no longer present in the controlled system until other coexisting orbits appear by the saddle-node bifurcation at $K \approx 0.72$.

3.3. Origin of Coexisting Orbits

The coexisting orbit keep unstable after the period-doubling route to chaos and the subsequent destruction of the generated chaotic attractor. The presence of the unstable coexisting orbits is here traced using numerical shooting methods for the periodic solutions of differential difference equations [21, 22]. Figure 4 shows that the branches of the coexisting period- 3τ orbit traced from the saddle-node bifurcation point to zero feedback gain. Black and gray branches show the trajectory of coexisting node and saddle, respectively.

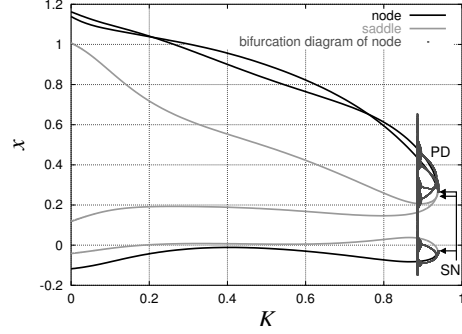


Figure 4: Continuation of coexisting period- 3τ orbit

At the upper limit of the stability range, the branches of the saddle and node coalesce and annihilate by the saddle-node bifurcation, as already mentioned in Sec.3.2.1. In the opposite side of the bifurcation point, all the branches develop at $K = 0$. Since the controlled system degenerates into two dimensional system at $K = 0$, we conclude that the coexisting orbits originate from unstable periodic orbits embedded in the chaotic attractor of the uncontrolled system. With the feedback gain approaching to zero, the characteristic multipliers of the coexisting orbits converge to zero except two multipliers because of the degeneration of the controlled system. The multipliers of the node is degenerated into $(-84.1594, 0)$ and $(-0.000095, 0)$. It implies that the orbit finally coincides with an inversely unstable period- 3τ orbit in the original system. As for the saddle, the multipliers are degenerated to $(247.724, 0)$ and $(-0.000007, 0)$, showing that the orbit coincides with a directly unstable period- 3τ orbit in the original system.

3.4. Relation between Existence of Coexisting Orbits and Remain of Chaos

The existence of the coexisting orbits estimates the remain of the original chaotic dynamics in the controlled system, which complicates the domain of attraction for the target orbits and causes long chaotic transient before stabilization [18]. This is because the coexisting orbits are derived from orbits embedded in the original chaotic attractor. The remain of the chaotic dynamics is here associated with the annihilation of the pair of the coexisting orbits by saddle-node bifurcation.

Figure 5 shows the unstable manifold¹ of a unstable period- τ orbit denoted by 1D . Here the 1D is a directly unstable periodic orbit, which cannot be stabilized by the control method because of the odd number condition. The unstable manifold is in function space and here projected on the two dimensional plane induced by stroboscopic mapping with period- 2π . It is well known that the uncontrolled system, which is effectively identical to the controlled system under $K = 0$, exhibits chaotic behavior, as results of the homoclinic intersection of the unstable manifold and the stable one from the same orbit 1D [19, 20]. The global phase structure of the controlled system is governed by the

¹The unstable manifold for $K > 0$ may not form a manifold in the sense of differential topology, because Eq. (1) including time delay may not have an unique backward solution for every initial condition [23, 24].

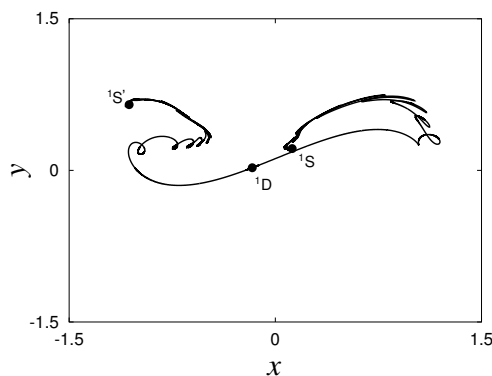


Figure 5: Unstable manifold of 1D at $K = 1.0$. The unstable manifold is projected from function space to the two dimensional plane which is obtained by stroboscopic observation with period- 2π .

presence of 1D , since the position and dynamical properties of the 1D are kept under the control.

Note that the coexisting period- 3τ orbits originate from the one embedded in the original chaotic attractor. Therefore, the annihilation of the orbits implies the disappearance of the original chaotic invariant set produced by the homoclinic intersection. In fact, one can easily confirm that the unstable manifold becomes a completely simple curve, as shown in Fig. 5, once the feedback gain is increased to 1.0 at which no coexisting orbits exists in the controlled system and thereby the homoclinic intersection unravels under the effect of the control signal. This result shows that the annihilation of the coexisting orbits gives a criterion for the disappearance of the original chaotic dynamics, which is possibly left under the small amplitude of the feedback gain.

4. Concluding Remarks

In this paper, multiple steady states have been discussed in the two-well Duffing system under time delayed feedback control. The multiple steady states occurs in the controlled system with the stabilization of the nontarget unstable periodic orbits originally embedded in the chaotic attractor. We showed that the annihilation of the coexisting orbits by saddle-node bifurcation indicates the disappearance of the original chaotic dynamics in the controlled system.

Acknowledgments

This research is supported by the Ministry of Education, Culture, Sports, Science and Technology in Japan, The 21st Century COE Program #14213201.

References

[1] H. G. Schuster, ed., "Handbook of Chaos Control," (Wiley-VCh, 1999).

- [2] E. Ott, C. Grebogi and A. Yorke, *Phys. Rev. Lett.*, vol.64, pp.1196–1199, 1990.
- [3] K. Pyragas, *Phys. Lett. A*, vol. 170, pp.421–428, 1992.
- [4] K. Pyragas and A. Tamasevicius, *Phys. Lett. A*, vol.204, pp.255–262, 1993.
- [5] S. Bielański, D. Derozier and P. Glorieux, *Phys. Rev. E*, vol.49, pp.R971–R974, 1994.
- [6] Th. Pierre, G. Bonhomme and A. Atipo, *Phys. Lett. A*, vol.76, pp.2290–2293, 1996.
- [7] T. Hikiyama and T. Kawagoshi, *Phys. Lett. A*, vol.211, pp.29–36, 1996.
- [8] P. Parmananda, R. Madrigal, M. Rivera, L. Nyikos, I. V. Kiss and V. Gáspár, *Phys. Rev. E*, vol.59, pp.5266–5271, 1999.
- [9] W. Just, E. Reibold, K. Kacperski, P. Fronczak, J. A. Holyst and H. Benner, *Phys. Rev. E*, vol.61, pp.5045–5056, 2000.
- [10] J. E. S. Socolar, D. W. Sukow and D. J. Gauthier, *Phys. Rev. E*, vol.50, pp.3245–3248, 1994.
- [11] K. Pyragas, *Phys. Lett. A*, vol.206, pp.323–330, 1995.
- [12] T. Ushio, *IEEE Trans. CAS-I*, vol.43, pp.815–816, 1996.
- [13] H. Nakajima and Y. Ueda, *Physica D*, vol.111, pp.143–150, 1998.
- [14] W. Just, T. Bernard, M. Ostheimer, E. Reibold and H. Benner, *Phys. Rev. Lett.*, vol.78, pp.203–206, 1997.
- [15] K. Pyragas, *Phys. Rev. Lett.*, vol.86, pp.2265–2268, 2001.
- [16] T. Hikiyama and Y. Ueda, *CHAOS*, vol.9, pp. 887–889, 1999.
- [17] K. Yamasue and T. Hikiyama, *Phys. Rev. E*, vol.69, 056209, 2004.
- [18] K. Yamasue and T. Hikiyama, in *XXI International Congress of Theoretical and Applied Mechanics*, Warsaw, Poland, August 15-21, 2004.
- [19] F. C. Moon and P. J. Holmes, *Journal of Sound and Vibration*, vol.65, pp.275–296, 1979.
- [20] Y. Ueda, H. Nakajima, T. Hikiyama and H. B. Stewart, in *Dynamical Systems Approaches to Nonlinear Problems in Systems and Circuits* (Eds. by Fathi M. A. Salam and Mark L. Levi), pp.128–137 (SIAM, Philadelphia, 1988).
- [21] T. Luzyanina, K. Engelborghs and K. Lust, *Int. J. of Bif. and Chaos*, vol.7, pp.2547–2560, 1997.
- [22] H. Ito and A. Kumamoto, *IEICE Trans. Fundamentals*, vol.E81-A, pp.1791–1797, 1998.
- [23] J. K. Hale, "Theory of Functional Differential Equations," (Springer-Verlag New York Inc., 1977).
- [24] J. K. Hale, L. T. Magalhães and W. M. Oliva, "Dynamics in Infinite Dimensions 2nd Ed.," (Springer-Verlag New York Inc., 2002).